



UNIVERSITY
OF WOLLONGONG
AUSTRALIA

University of Wollongong
Research Online

Faculty of Science, Medicine and Health - Papers

Faculty of Science, Medicine and Health

2015

Treatment of RO brine from CSG produced water by spiral-wound air gap membrane distillation - a pilot study

Hung Duong

University of Wollongong, chd581@uowmail.edu.au

Allan Chivas

University of Wollongong, toschi@uow.edu.au

Bart Nelemans

AquaStill

Mikel C. Duke

Victoria University

Stephen Gray

Victoria University

See next page for additional authors

Publication Details

Duong, H. C., Chivas, A. R., Nelemans, B., Duke, M., Gray, S., Cath, T. Y. & Nghiem, L. D. (2015). Treatment of RO brine from CSG produced water by spiral-wound air gap membrane distillation - a pilot study. *Desalination*, 366 121-129.

Research Online is the open access institutional repository for the University of Wollongong. For further information contact the UOW Library:
research-pubs@uow.edu.au

Treatment of RO brine from CSG produced water by spiral-wound air gap membrane distillation - a pilot study

Abstract

Brine management is a major bottleneck for coal seam gas (CSG) production in Australia. This study investigated the concentration of CSG reverse osmosis (RO) brine using a pilot membrane distillation (MD). The system was equipped with a novel spiral-wound air gap membrane distillation (AGMD) module. By operating the pilot MD system at low feed temperature and a small temperature gradient, a stable distillate production rate could be maintained. The resulting low permeate flux can be offset by a high packing density of the spiral-wound membrane module. Here, using a module with diameter, height, and total membrane surface area of 0.4 m, 0.5 m, and 7.2 m², respectively, the pilot MD system sustainably achieved 80% water recovery and produced 10 L/h of distillate from CSG RO brine. Overall, 95% water recovery could be obtained from CSG produced water for beneficial uses by a combination of RO and AGMD without any observable membrane scaling. A preliminary thermal energy demand analysis suggests that if installed in New South Wales (Australia), 1 ha of flat-plate solar thermal collector arrays could provide sufficient thermal energy to treat 472 m³/day (2970 bbl/day) of CSG produced water using the proposed RO/AGMD treatment train.

Disciplines

Medicine and Health Sciences | Social and Behavioral Sciences

Publication Details

Duong, H. C., Chivas, A. R., Nelemans, B., Duke, M., Gray, S., Cath, T. Y. & Nghiem, L. D. (2015). Treatment of RO brine from CSG produced water by spiral-wound air gap membrane distillation - a pilot study. *Desalination*, 366 121-129.

Authors

Hung Duong, Allan Chivas, Bart Nelemans, Mikel C. Duke, Stephen Gray, Tzahi Y. Cath, and Long D. Nghiem

Treatment of RO brine from CSG produced water by spiral-wound air gap membrane distillation – a pilot study

Revised Manuscript Submitted to

Desalination

Special Issue: Energy and Desalination

Hung C. Duong¹, Allan R. Chivas², Bart Nelemans³, Mikel Duke⁴, Stephen Gray⁴, Tzahi Y. Cath⁵, Long D. Nghiem^{1,*}

¹ Strategic Water Infrastructure Laboratory, School of Civil Mining and Environmental Engineering, University of Wollongong, Wollongong, NSW 2522, Australia

² GeoQuEST Research Centre, School of Earth & Environmental Sciences, University of Wollongong, NSW 2522, Australia

³ AquaStill, Nusterweg 69, 6136 KT Sittard, The Netherlands

⁴ Institute for Sustainability and Innovation, Victoria University, Australia

⁵ Advanced Water Technology Center (AQWATEC), Department of Civil and Environmental Engineering, Colorado School of Mines, Golden, CO 80401, USA

* Corresponding author: Long Duc Nghiem, Email longn@uow.edu.au; Tel: +61 2 4221 4590

RESEARCH HIGHLIGHTS

- Pilot treatment of CSG water by a combination of UF/RO and AGMD was demonstrated.
- An overall water recovery of 95% was achieved over a sustained period.
- The precipitation of Si and Ca may lead to scaling in long term operation.
- One ha of land can provide solar thermal for treating 118 m³/d of CSG RO brine.

Abstract: Brine management is a major bottleneck for coal seam gas (CSG) production in Australia. This study investigated the concentration of CSG reverse osmosis (RO) brine using a pilot membrane distillation (MD). The system was equipped with a novel spiral-wound air gap membrane distillation (AGMD) module. By operating the pilot MD system at low feed temperature and a small temperature gradient, a stable distillate production rate could be maintained. The resulting low permeate flux can be offset by a high packing density of the spiral-wound membrane module. Here, using a module with diameter, height, and total membrane surface area of 0.4 m, 0.5 m, and 7.2 m², respectively, the pilot MD system sustainably achieved 80% water recovery and produced 10 L/h of distillate from CSG RO brine. Overall, 95% water recovery could be obtained from CSG produced water for beneficial uses by a combination of RO and AGMD without any observable membrane scaling. A preliminary thermal energy demand analysis suggests that if installed in New South Wales (Australia), one hectare of flat-plate solar thermal collector arrays could provide sufficient thermal energy to treat 472 m³/day (2970 bbl/day) of CSG produced water using the proposed RO/AGMD treatment train.

Keywords: Coal seam gas (CSG) produced water; air gap membrane distillation (AGMD); brine management; water recovery.

1 Introduction

Coal seam gas (CSG) – known as coal seam methane or coal bed methane in the US and Canada – has emerged as an important source of energy in many countries. CSG is essentially methane gas produced in coal seams at up to about 1,000 m depth, where it is trapped in fractures and on the surface of the coal. Similar to coal, the geographical distribution of CSG is much more dispersed than that of oil and conventional natural gas. The ultimately recoverable CSG reserve has only been estimated for Europe, North America, and Asia-Pacific where sufficient geological data are available. It already amounts to about 120 trillion m³ or about 25% of the current global conventional natural gas reserve [1].

CSG production is commonly accompanied by the undesired co-extraction of a large volume of water to the surface. This water is known as CSG produced water, and in Australia, it is rich in sodium, bicarbonate, and chloride. Thus, CSG produced water is usually saline and sodic and must be treated prior to environmental discharge or beneficial use [2-4]. The volume of produced water associated with CSG production for some basins is enormous. For example, the annual generation of CSG produced water from Southern Queensland alone is expected to be 175 GL/year, spanning until 2060 to result in an accumulative volume of 5,100 GL [5]. Therefore, cost-effective and sustainable management of this large volume of produced water is of paramount importance to the CSG industry around the world.

The current state-of-the-art CSG produced water treatment system involves pretreatment (e.g., coagulation, microfiltration (MF) or ultrafiltration (UF), and in some cases ion exchange) followed by reverse osmosis (RO) desalination [2, 6-8]. The desalted water can be used for a range of beneficial purposes including coal washing, dust suppression, irrigation, livestock watering, industrial consumption, and even drinking water supply [2, 7, 9]. RO can only achieve 75 – 80% water recovery and it is still necessary to manage the RO brine, which is 20 – 25% of the initial CSG produced water volume. This CSG RO brine presents a vexing challenge to the CSG industry and environmental regulators. In the absence of any technically and economically proven processes for CSG RO brine management, it is being stored in brine ponds. Brine storage is an expensive, temporary, and environmentally risky option until the water sector can catch up with the rapid growth of the CSG industry. In fact, in Australia, the state of Queensland has established a CSG produced water management policy to encourage the extraction of usable products from the brine wherever possible as a procedure to gradually phase out the use of brine ponds for indefinite storage [10]. In addition, while reinjection of CSG produced water or brine to coal seams can be considered in the US and several other countries, it is generally not allowed in Australia.

Several CSG brine utilisation techniques have been proposed in recent years [8]. For example, Penrice in collaboration with General Electric (GE, Australia) and QGC (QGC Pty Limited, Australia) has announced a pilot project to demonstrate the recovery of soda ash from CSG brine rich in sodium bicarbonate [11]. Another notable approach is to use saturated CSG brine as feed stock for the production of sodium hydroxide [12]. While the proof of concept of these approaches has been demonstrated, a critical step is to further concentrate CSG RO brine to near the point of saturation. Traditional thermal distillation processes such as multi-stage flash, multi-effect distillation, and vapour compression can be used for this step; however, they are notorious for their large physical and energy footprint as well as high capital cost [13]. In this context, membrane distillation (MD), which is a thermally driven membrane process, can be an ideal alternative to the thermal distillation processes for further concentrating CSG RO brine.

The MD process involves the phase conversion from liquid to vapour on one side of the membrane and the condensation of vapour to liquid on the other side [14]. In MD, a hydrophobic microporous membrane is used to facilitate the transport of water vapour through its pores. As a result, the MD process is more compact and has a smaller footprint than traditional thermal distillation processes [15, 16]. Moreover, because water is transported through the membrane only in the vapour phase, in theory 100% or near complete rejection of ions and dissolved non-volatile organics can be achieved. In addition, unlike in RO filtration, due to the discontinuity of the liquid phase across the membrane, in the MD process the mass flux is not significantly affected by the transmembrane osmotic pressure difference. As a result, the greatest potential of MD can be realised for the treatment of highly saline solutions [16-19].

Integrated desalination systems in which MD is used to further enhance water recovery have been extensively studied [20-25]. Drioli et al. [20] integrated MD into a combined MF/UF/RO sea water desalination process. RO brine with total dissolved solids (TDS) of 75 g/L was further treated by MD to increase the overall fresh water recovery up to 88%. Adham et al. [21] reported a feasible and effective MD process capable of treating the brine from a thermal desalination plant with high salinity of 70 g/L TDS. Distillate of excellent quality (conductivity below 10 $\mu\text{S}/\text{cm}$) was produced. Ji et al. [22] investigated the treatment of seawater RO brine by a MD-crystallisation hybrid process and demonstrated an overall fresh water recovery of up to 90% as well as the production of sodium chloride crystals. It is, however, noteworthy that no previous studies have explored the use of MD for the treatment of CSG RO brine. Therefore, this study aims to demonstrate and evaluate the performance of a pilot air gap membrane distillation (AGMD) system for further volume reduction of CSG RO brine.

2 Materials and Methods

2.1 Pilot MD system

A pilot MD system from AquaStill (Sittard, The Netherlands) was used in this study (Fig. 1). The pilot MD system consisted of a spiral-wound AGMD membrane module, a feed water tank, a water-circulating pump, temperature and pressure sensors, and a flow meter. The membrane module contained 7.2 m² of low-density polyethylene membrane having nominal pore size of 0.3 μm, thickness of 76 μm, and porosity of 85%. Key characteristics of the membrane module are provided in Table 1. The pilot MD system was equipped with a supervisory control and data acquisition system, which was used to regulate the water circulation flow rate and temperature of the hot feed water entering the evaporator channels of the membrane module.

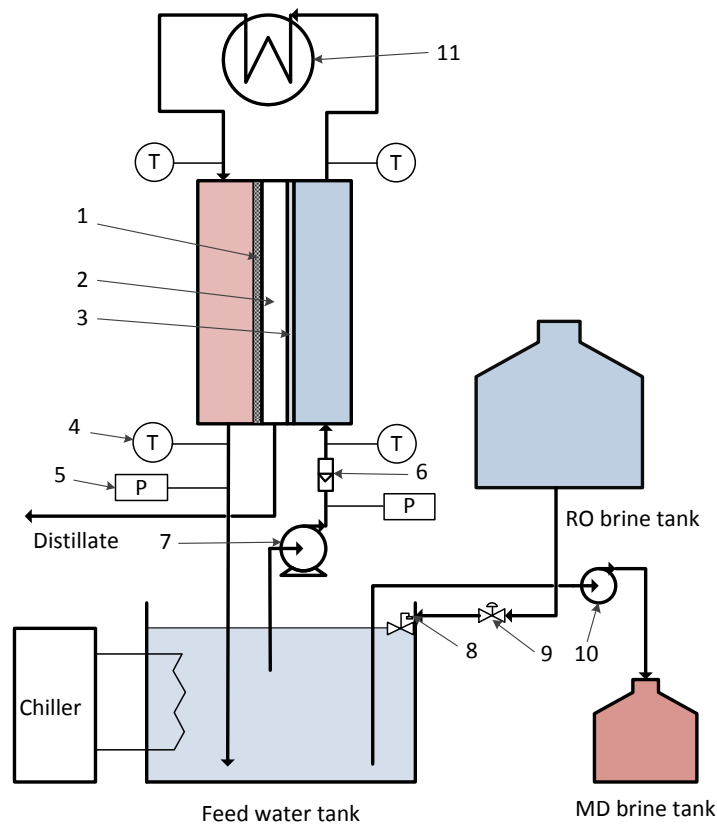


Fig. 1. Schematic diagram of the CSG RO brine treatment by the pilot MD system: (1) membrane, (2) air gap, (3) condenser, (4) temperature sensors; (5) pressure sensors, (6) flow meter, (7) water-circulating pump, (8) float valve, (9) one-way valve, (10) peristaltic pump, (11) heat exchanger.

A novel aspect of this study is the use of the spiral-wound AGMD module, which is more energy efficient compared to most other MD configurations. In the AGMD module, a condenser is inserted between the membrane and the coolant stream to create a stagnant air gap. As a result, the heat loss due to conduction through the membrane can be attenuated and is much smaller than that in direct contact membrane distillation [26, 27]. More importantly, because the coolant stream is separated from the hot water vapour by the condenser, internal recovery of the latent heat of condensation is possible in AGMD. It is noteworthy that AGMD is normally operated at a low permeate flux because of a small temperature gradient across the membrane. The spiral-wound membrane module used in this study has a packing density of $115 \text{ m}^2/\text{m}^3$ and thus can offset the low permeate flux of this operating regime.

Table 1. Characteristics of the spiral-wound AGMD module.

Total net membrane surface area (m^2)	7.2
Diameter of the module (m)	0.4
Height of the module (m)	0.5
Length of envelope (m)	1.5
Width of envelope (m)	0.4
Thickness of flow channels (mm)	2.0
Number of evaporator channels	6
Number of condenser channels	6
Number of distillate channels	12

RO brine was fed into the MD feed water tank by gravity via a float valve. An external chiller was used to reduce the temperature in the feed tank in this study; however, in practice, raw CSG water can be used as a heat sink. As schematically depicted in Fig. 1, the CSG RO brine was pumped into the condenser inlet of the AGMD module and was initially used as the coolant fluid. As this cool CSG RO brine was flowing through the condenser channels, it was pre-heated by the latent heat from vapour condensation. After leaving the module, the pre-heated CSG RO brine feed water was further heated using a heat exchanger to reach the desired MD feed temperature. In practice, this additional heat may be sourced from solar thermal collectors, waste heat associated with electricity generation, and the liquefaction of natural gas. The heated CSG RO brine feed water then entered the evaporator channels and travelled through the module in the reverse direction. As the heated CSG RO brine travelled along the evaporator channels, water vapour diffused through the membrane pores and the brine was cooled. The cool brine was returned to the feed water tank to start another cycle.

2.2 Pilot UF/RO treatment

The CSG produced water used in this study was from a pilot gas well in Gloucester, New South Wales (Australia). A pilot UF/RO system provided by Osmoflo (Adelaide, SA, Australia) was used to produce CSG RO brine for the pilot MD investigation (Fig. 2). CSG produced water was pre-treated by UF and then desalted by RO to achieve 75% water recovery. The brine (which is 25% of the initial CSG produced water volume) from RO was fed into the pilot MD system for brine volume reduction and further fresh water extraction. The pilot UF system was equipped with two hollow fibre polyacrylonitrile membrane modules (Ultra-Flo U860, Singapore) with a total membrane surface of 96.6 m² and was operated in dead end mode. The pilot RO system consisted of three 4-inch spiral-wound membrane modules (AG4040FM, General Electric, CT, USA) having a total membrane surface of 71.1 m². Anti-scalant (Osmotreat, Osmoflo, Adelaide, SA, Australia) was added to the CSG water just before the RO treatment at a dosage of 5 mg/L.

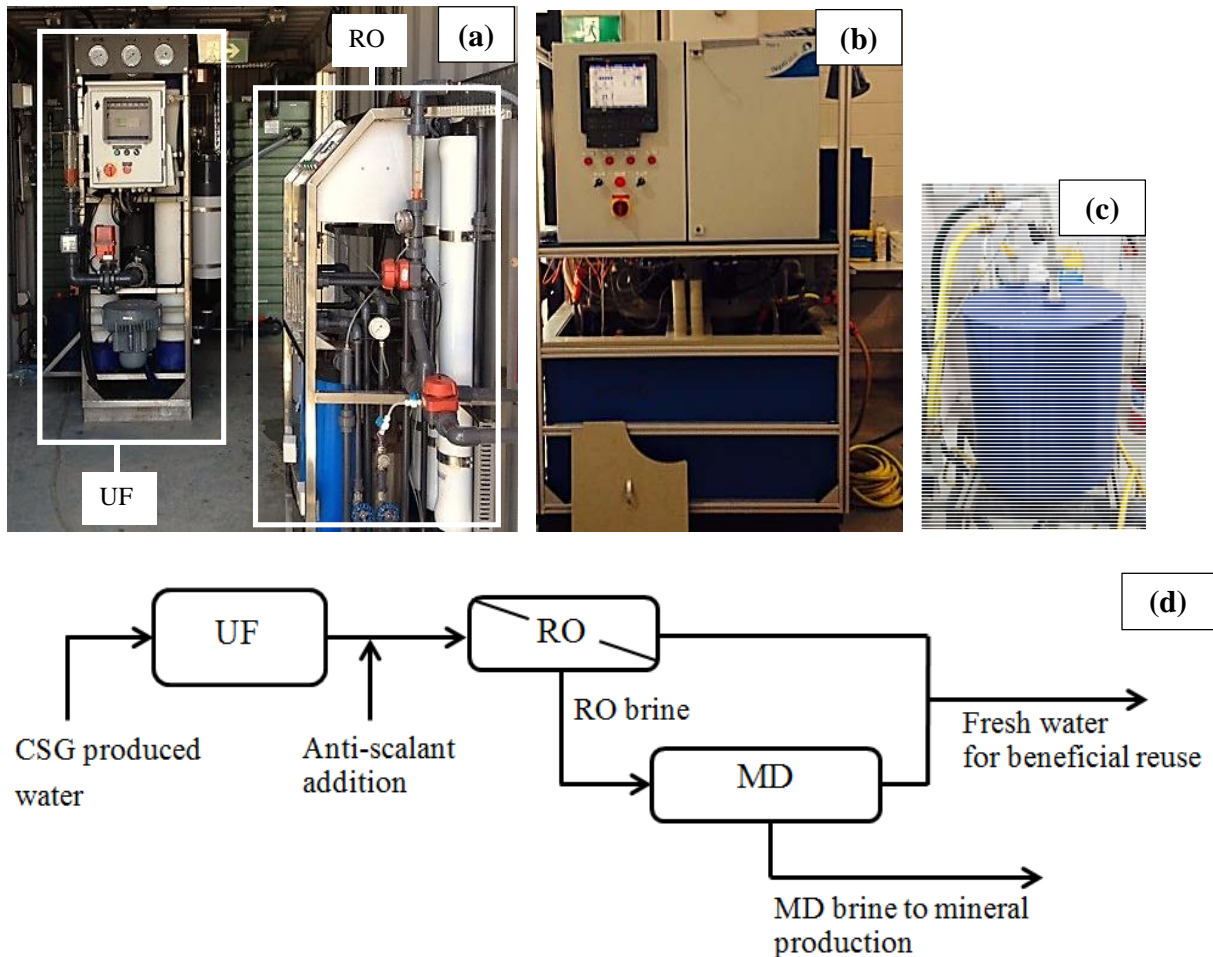


Fig. 2. The treatment process of CSG produced water; (a) UF and RO pilot systems, (b) MD pilot system, (c) Spiral-wound AGMD membrane module, (d) Schematic diagram of the treatment process.

2.3 Energy consumption and thermal efficiency calculations for the pilot MD system

In the pilot MD process, thermal energy was used for heating the RO brine entering the evaporator channels and cooling the water in the feed tank, while electrical energy was required to operate the water-circulating pump. It is noteworthy that an external chiller was used in this pilot study; however, the available CSG produced water can be used as the heat sink via a heat-exchanging system. Thus, the thermal energy consumption of the pilot MD system was evaluated based on the thermal energy required to heat the CSG RO brine. To assess the thermal energy consumption of the pilot MD system, the specific thermal energy consumption (STEC) (kWh/m³), which is the amount of heat consumed to generate 1 m³ of MD distillate, was calculated using Eq. (1) [28, 29]:

$$\text{STEC} = \frac{Q_{\text{in}}}{J} = \frac{m_f \cdot C_p \cdot (T_{\text{ein}} - T_{\text{cout}})}{J} \quad (1)$$

where Q_{in} is the rate of total heat input to the system (kW), J is the MD distillate production rate (m³/h), m_f is the mass flow rate of feed water (kg/h), C_p is the specific heat capacity of feed water (kWh/kg.K), T_{cout} is the temperature of feed water leaving the condenser channels (K), and T_{ein} is the temperature of feed water flowing into the evaporator channels of the AGMD membrane module (K).

To evaluate the thermal efficiency of the MD system, the gained output ratio (GOR) was calculated using Eq. (2) [29, 30]:

$$\text{GOR} = \frac{m_d \cdot \Delta H_v}{Q_{\text{in}}} \quad (2)$$

where m_d is the MD distillate mass flow rate (kg/h) and ΔH_v is the latent heat of evaporation of water (kWh/kg).

In MD processes, heating and cooling consume the major fraction of the supplied energy, thus the actual electrical energy consumption is commonly overlooked in the literature. However, electrical energy consumption is also important and must be known. In this study, the electrical energy consumption of the pilot MD system was estimated using the specific electrical energy consumption (SEEC) (kWh/m³), which is the amount of electrical energy required to produce 1 m³ of MD distillate. Eq. (3) was used to calculate the SEEC of the pilot MD system [31]:

$$\text{SEEC} = \frac{F \cdot \Delta P}{36000 \cdot \eta \cdot J} \quad (3)$$

where F is the water circulation flow rate (L/h), ΔP is the hydraulic pressure drop over the AGMD module (bar), and η is the efficiency of the water-circulating pump.

2.4 Analytical methods

2.4.1 Anion analysis

The concentrations of anions were determined using an ion chromatograph (LC-20AC, Shimadzu, Kyoto, Japan) that was equipped with a Dionex IonPac AS23 anion-exchange column (Thermo Scientific, Waltham, Massachusetts, USA). A solution containing 4.5 mM Na_2CO_3 and 0.8 mM NaHCO_3 was used as the eluent. The sample injection volume and eluent flow rates were 10 μL and 1 mL/min, respectively. Prior to analysis, the system was calibrated using standard solutions containing 5, 10, 50, and 100 mg/L of each ion.

2.4.2 Cation analysis

The concentrations of cations were analysed using an Agilent 7500CS ICP-MS (Agilent Technologies, Wilmington, DE, USA). A lithium internal standard (BDH Spectrosol, Poole, U.K.) was spiked to all samples at a concentration of 4 $\mu\text{g/L}$. Sample dilution was carried out with 5% Suprapur nitric acid with a dilution factor of up to 20. Calibration was conducted prior to each batch of analysis. The linear regression coefficients for all calibration curves were greater than 0.99 for all elements. Prior to each batch of analyses, the ICP-MS was tuned by a multi-element tuning solution that contained 10 $\mu\text{g/L}$ of Li, Y, Ce, Tl, and Co. Each analysis was conducted in triplicate and the variation was less than 5% [32].

Electrical conductivity and pH of MD distillate and brine were measured using an Orion 4-Star Plus pH/conductivity meter (Thermo Scientific, Waltham, Massachusetts, USA).

2.5 Experimental protocols

Operation of the pilot MD system was first optimised in the laboratory using an 8000 mg/L sodium chloride feed solution. The aim of this test was to optimise the water circulation flow rate and operating temperature as well as to identify the separation performance of the system. During the preliminary tests, tap water was continuously added to the feed tank via the float valve to compensate for the distillate flow and to maintain a constant feed salinity.

Optimising the water circulation flow rate was necessary. A high circulation flow rate can be used to minimise membrane scaling and temperature polarisation on the membrane surface. However, there are several limitations to the circulation flow rate in the pilot MD system. First, the spiral-wound AGMD module used in this study was designed to utilise the internal heat recovery of the system. The latent heat of condensation is recovered from the hot vapour to the coolant through the condenser foil. Hence, sufficient contact time is required for effective heat

recovery. Second, an excessive circulation flow rate can cause high pressure inside the module leading to intrusion of liquid into the membrane pores causing contamination of the distillate. Lastly, a rise in circulation flow rate results in increased pumping and, in turn, an increase in the electrical energy consumption. Due to the long path for water travelling through the module, there exists a significant hydraulic pressure drop between the inlet and outlet of the module, and at a high circulation flow rate the pressure drop can be significant. Thus, the maximum differential pressure between the inlet and outlet was set at 0.7 bar (10 psi).

After the initial optimisation process, the pilot MD system was deployed at a CSG site in Gloucester, New South Wales (Australia), for further testing. The pilot MD was initially operated only during the daytime to allow close supervision. At the end of each day, the AGMD module was disconnected from the system to completely drain all residual liquid. During this initial intermittent operation, the increase in salinity of the CSG brine in the feed tank due to distillate extraction was monitored by electrical conductivity measurement. When the feed CSG RO brine in the feed tank concentrated by a factor of 5 (i.e., 80% water recovery), the pilot MD was switched to automatic and continuous operation mode for the remainder of the pilot program. A peristaltic pump was used to remove excess MD brine from the feed tank (Fig. 1). The excess MD brine pumped-out flow rate was 25% of the distillate flow rate to maintain a water recovery of 80%. The electrical conductivities, pH, and flow rates of MD brine and distillate were monitored and recorded on a regular basis.

3 Results and discussion

3.1 UF/RO treatment of CSG produced water

The CSG produced water used in this study can be characterised as slightly saline, highly sodic, and rich in sodium, bicarbonate and chloride. Key characteristics and ionic composition of the CSG produced water are summarised in Table 2. The average electrical conductivity and sodium adsorption ratio (SAR), which is a measure of the water sodicity [2], of the CSG produced water were 6,550 $\mu\text{S}/\text{cm}$ and 103, respectively. Given these values, the CSG produced water could pose detrimental impacts on soil structure and the growth of plants; therefore, it was not suitable for irrigation or direct environmental discharge [2, 9].

The combined UF/RO system operated sustainably at a water recovery of 75% from CSG produced water. No evidence of membrane fouling or scaling was observed during the pilot program. At 75% water recovery, the UF/RO system produced more RO brine than the MD system could accommodate. Thus, the UF/RO system was only operated intermittently. The RO permeate was of high quality (Table 2) and suitable for a range of beneficial uses.

Table 2. Characteristics of water before and after the pilot UF/RO treatment of CSG produced water.

	Raw CSG water	RO permeate	RO brine
General characteristics			
Conductivity ($\mu\text{S/cm}$)	6,550	110	21,800
Total dissolved solids (g/L)	3.57	0.06	14.10
Turbidity (NTU)	6.1	0.07	0.22
pH	8.2	6.8	8.2
SAR	103	-	-
Ion concentration (mg/L)			
Sodium	1,710	18	6,840
Bicarbonate	1,920	0	4,740
Chloride	1,400	15	5,520
Magnesium	5	0	17
Potassium	8	0	32
Calcium	10	1	14
Iron	0	0	0
Silica	13	1	75

3.2 Characteristics of the pilot MD system

The differential hydraulic pressure between the membrane module inlet and outlet was over the permissible maximum value (0.7 bar) when the circulation flow rate was increased above 450 L/h. Thus, the pilot MD was evaluated at the circulation flow rates of 350, 400, and 450 L/h (cross flow velocities of 0.020, 0.023, and 0.026 m/s, respectively).

As discussed in Section 2.1, the MD feed solution was introduced to the membrane module first as the coolant fluid to recover the heat of condensation, and after being further heated as the actual feed to the evaporator channels. Therefore, the effective temperature difference across the membrane reported here was much lower than that in a laboratory-scale module with a small membrane surface area [33]. Nevertheless, an increase in the feed solution temperature immediately before entering the evaporator channels could also lead to an increase in the bulk temperature difference (ΔT) between the hot and cold streams along the membrane channels (Fig. 3). As a result, there was a notable rise in the distillate production rate when the evaporator inlet temperature increased from 50 to 60 °C (corresponding to an increase in ΔT from 3.1 to 3.9 °C). It is noteworthy that, under all experimental conditions evaluated here, ΔT values at the entrance and exit of the module were identical. However, the transmembrane temperature difference inside the membrane module could be influenced by temperature polarisation [34]. The distillate production rate also increased with increasing circulation flow rate. This can be attributed to a

decrease in temperature polarisation on the membrane surface, which is an intrinsic phenomenon in MD [35]. In fact, the impact of circulation flow rate on the distillate production rate was more prominent as the evaporator inlet temperature (and thus temperature polarisation) increased (Fig. 3).

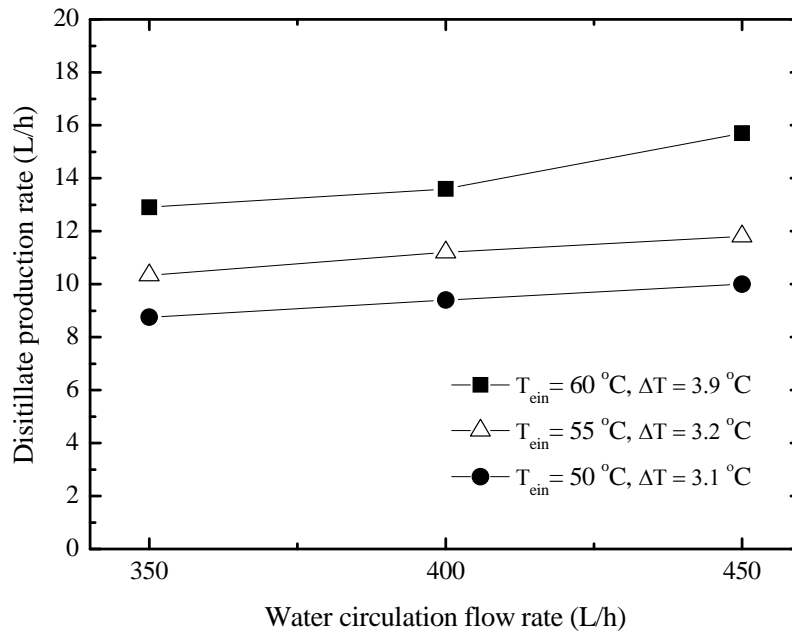


Fig. 3. Distillate production rate of the pilot MD system at various evaporator inlet temperatures (T_{ein}) and water circulation flow rates. Feed solution was 8000 mg/L sodium chloride.

The increase in both evaporator inlet temperature and circulation flow rate resulted in a small increase in salinity leakage; however, the distillate conductivity was still very low. Even at the highest evaporator inlet temperature (60 °C) and circulation flow rate (450 L/h), the distillate conductivity was less than 60 $\mu\text{S}/\text{cm}$, resulting in a conductivity rejection of over 99.5%. Overall, the influence of operating conditions on the conductivity rejection by the pilot MD system was negligible.

The water permeate flux achieved during the preliminary tests with 8000 mg/L sodium chloride feed solution was low, ranging from 1.2 to 2.2 $\text{L}/\text{m}^2\text{h}$, depending on the operating conditions. However, given the high packing density of the spiral-wound AGMD module (i.e. 115 m^2/m^3), distillate production rate in the range of 8.5 to 16 L/h could be obtained in this study.

3.3 Treatment of CSG RO brine by the pilot MD system

Based on the initial assessment of the impact of operating conditions on distillate production rate, the highest circulation flow rate (450 L/h) was selected to evaluate the treatment of CSG RO brine to minimise the risk of membrane scaling. On the other hand, the intermediate evaporator inlet temperature of 55 °C was chosen to balance between a low scaling potential (which increases with temperature) and a high distillate production rate.

During the treatment of CSG RO brine, there were some variations in system performance in comparison with the initial assessment using the synthetic sodium chloride feed solution. Of particular note, a ΔT of approximately 4 °C was obtained at the evaporator inlet temperature and the condenser inlet temperature of 55 and 25 °C, respectively, and the distillate production rate showed two major trends consistent with two operation modes (Fig. 4).

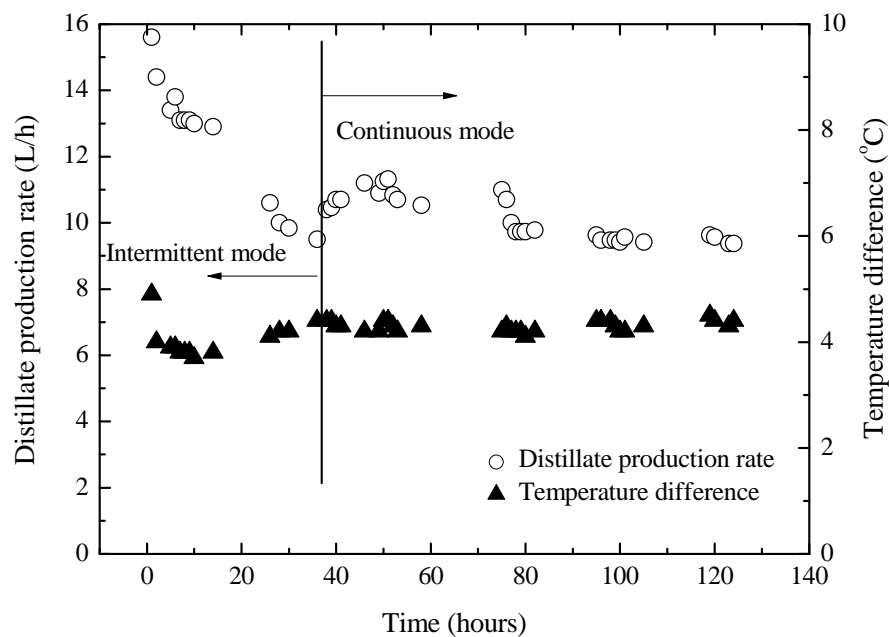


Fig. 4. Distillate production rate and temperature difference as a function of time during the pilot MD treatment process of CSG RO brine (The condenser inlet temperature $T_{cin} = 25$ °C; the evaporator inlet temperature $T_{ein} = 55$ °C; water circulation flow rate $F = 450$ L/h).

A gradual decrease in distillate production rate was observed during intermittent operation. Initially, the distillate production rate of the system was 15 L/h (permeate flux of 2.1 L/m²h), and then it gradually decreased to 10 L/h (permeate flux of 1.4 L/m²h) as the concentration factor

increased to 5. There could be several reasons for this reduction in the distillate production rate with increasing feed concentration.

First, increased feed solution salinity resulted in a decrease in water activity, thus, reducing the transmembrane partial vapour pressure difference, which is the driving force of the MD process [14]. As a result, the distillate production rate decreased with increasing feed salinity. Indeed, using the Antoine equation [26], the calculated vapour pressure across the membrane decreased by 34% (at the assumed temperature polarisation coefficient of 0.5) when a feed solution containing 14 g/L of sodium chloride (equivalent to the TDS of the RO brine used here) was concentrated by 5 times.

Second, the increase in feed concentration led to a rise in the viscosity of the feed water and hence temperature polarisation, which subsequently reduced the rate of distillate production. In the pilot system, at the circulation flow rate of 450 L/h, the velocity of water travelling through the evaporator and condenser channels was low (0.026 m/s), and thus the temperature polarisation effect was significant. The considerable effect of the temperature polarisation on the distillate production rate was also proved in the evaluation of the pilot MD system during the optimising experiments.

Lastly, the release of carbon dioxide during the distillation process could also contribute to the reduction in the distillate production rate. The bicarbonate content of the RO brine was 4740 mg/L (Table 3). At elevated temperature, bicarbonate partly decomposed into carbonate and carbon dioxide ($2\text{HCO}_3^- = \text{CO}_3^{2-} + \text{CO}_2 + \text{H}_2\text{O}$) [36]. The transport of carbon dioxide through the membrane pores could compete with water vapour, thus, reducing the distillate production rate. In addition, the existence of carbon dioxide in gas phase in the evaporator channels reduced the effective membrane surface area for evaporation, resulting in the reduction in the distillate production rate. In fact, the release of carbon dioxide as gas bubbles was observed in the feed water tank at the brine-returning outlet. Furthermore, when CSG RO brine was used as the feed, the conductivity of the distillate was as high as 500 $\mu\text{S}/\text{cm}$, most of this could be attributed to bicarbonate.

Once the concentration factor of 5 had been reached (equivalent to 80% recovery), the MD system was operated continuously until the end of the pilot program and the feed salinity remained constant at about 80 mS/cm. As a result, a stable distillate production rate of 10 L/h could be achieved (Fig. 4). The anti-scalant added to the CSG produced water prior the RO process remained in the RO brine and may have prevented sparingly soluble salts from depositing on the membrane [21, 37]. In addition to the anti-scalant dosage, it is possible that the intentional system operation at low feed temperature and a small temperature gradient, and hence low water

flux (1.4 L/m²h in continuous operation), could reduce membrane scaling [38]. At a low permeate flux, the concentration polarisation, which would accelerate the precipitation of scale, was attenuated, reducing the risk of membrane scaling.

Table 3. Characteristics of water before and after the pilot MD treatment of CSG RO brine.

	RO brine	MD distillate	MD brine	Concentration Factor
General characteristics				
Conductivity (mS/cm)	21.8	0.5	82.1	4
Total dissolved solids (g/L)	14.10	0.25	86.10	6.1
Turbidity (NTU)	0.22	0.11	0.67	-
pH	8.2	6.3	8.2	-
Ion concentration (mg/L)				
Sodium	6,840	65	34,200	5
Bicarbonate	4,740	110	32,800	6.9
Chloride	5,520	63	31,800	5.8
Magnesium	17	nd	74	4.4
Aluminium	nd	nd	nd	-
Potassium	32	1	146	4.6
Calcium	14	nd	34	2.4
Iron	nd	nd	nd	-
Silica	75	5	170	2

nd: not detectable.

On the other hand, the ion concentration analyses (Table 3) revealed that potential scalants (silica and calcium) in the MD feed water may pose a scaling risk. Indeed, the concentrations of silica and calcium in the MD brine were lower than those calculated when the feed solution was concentrated by 5 times. Data reported here suggest that the co-precipitation of silica and calcium carbonate has possibly occurred on the internal surface of the heat exchanger used for heating MD feed water prior to entering the evaporator channels. Due to its inverse solubility to temperature, the risk of calcium carbonate scaling was highest in the heat exchanger where the maximum temperature occurred. Thus, the precipitation is likely to start from the heat exchanger. The scale deposition on the surface of the heat exchanger could reduce its efficiency (which was assessed by monitoring the temperature difference between the condenser outlet and the evaporator inlet). However, due to the slow kinetics of scale deposition, the effect of scale deposition on the efficiency of the heat exchanger was found insignificant over one week of continuous treatment.

Results reported here suggest that operating the pilot MD system at a low permeate flux (1.4 L/m²h) together with anti-scalant addition prior to RO treatment could be an effective measure to control membrane fouling. However, due to the complex and highly variable composition of the

CSG RO brine, further studies on membrane scaling during MD treatment of CSG RO brine are recommended.

Overall, the pilot MD system showed excellent separation performance even at a high water recovery. Conductivity rejection was always above 99.0% (Fig. 5). At the beginning of the experiment, the distillate conductivity was 100 $\mu\text{S}/\text{cm}$, and then increased sharply to 600 $\mu\text{S}/\text{cm}$ potentially due to the carbon dioxide permeation effect discussed earlier. During the continuous-mode operation, the water recovery was 80% and the distillate conductivity was stable at 500 $\mu\text{S}/\text{cm}$ (Fig. 5).

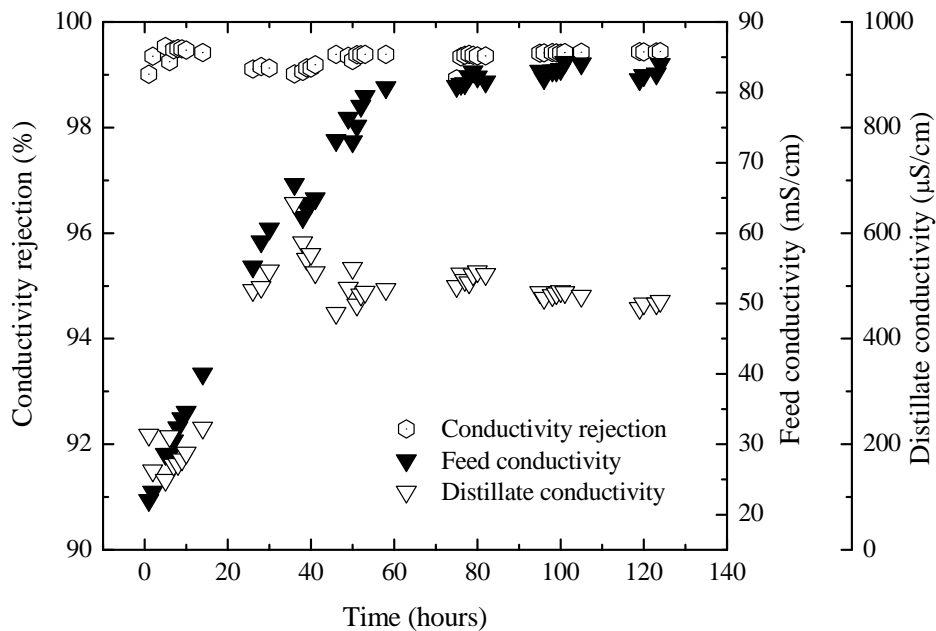


Fig. 5. Conductivity rejection of the pilot MD system and conductivities of its feed and distillate during the treatment of CSG RO brine.

It is worth noting that when using CSG RO brine, the salinity rejection (>99.0%) by the pilot MD system was slightly lower than that observed during testing with synthetic sodium chloride feed solution (99.5%). This slightly lower rejection when desalting CSG RO brine could be attributed to the permeation of carbon dioxide into the distillate, which also resulted in a much lower pH in the distillate compared to the feed (Table 3). Furthermore, there was also evidence that some carbon dioxide had escaped into the atmosphere. Indeed, at the continuous-mode operation (80% water recovery), the measured MD brine electrical conductivity of 82.1 mS/cm was significantly

less than the mass balance calculated value of 109 mS/cm (which was based on feed conductivity of 21.8 mS/cm and a concentration factor of 5).

3.4 Feasibility consideration

The thermal energy requirement of the pilot MD system in the treatment of RO brine from CSG produced water was evaluated using the STEC value, while its thermal efficiency was assessed by the GOR value. Fig. 6 shows the evolution of GOR, STEC, and the distillate production rate as a function of time. Values reported in this study are consistent with previous pilot MD studies [29] using other saline feed solutions (Table 4).

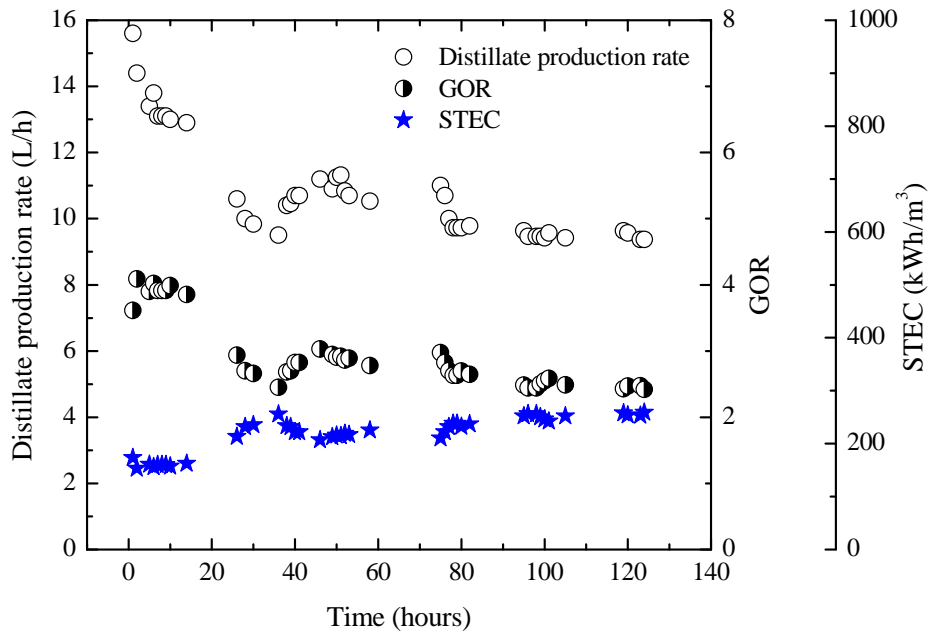


Fig. 6. Distillate production rate, GOR, and STEC as a function of time during the treatment of CSG RO brine by the pilot MD system ($T_{\text{cin}} = 55\text{ }^{\circ}\text{C}$, $T_{\text{cin}} = 25\text{ }^{\circ}\text{C}$, $F = 450\text{ L/h}$).

A correlation between GOR and the distillate production rate could be observed as expected from Eq. (2). Initially, at the distillate production rate of 15 L/h, the pilot MD system had a GOR value of 4. As the distillate production rate decreased because of the increased water recovery rate, GOR gradually decreased. GOR was then stable at about 2.5 throughout the continuous-mode operation when the distillate production rate remained steady at 10 L/h.

Table 4. Comparisons between the pilot MD system used in the present study and other pilot MD systems reported in literature.

	Present study	Literature			
		[42]	[43]	[28]	[44]
Permeate flux (L/m ² h)	2.1	2.1	2.5	3.4	1.88
Water circulation flow rate (L/h)	450	280-415	400	500	200-400
Feed temperature at evaporator inlet (°C)	55	60-85	-	85	60-85
STEC (kWh/m ³)	175-250	100-200	200-300	250-600	140-200
GOR	2.5-4	3-6	0.3-0.9	-	4-6

The STEC of the pilot MD system was also linked to GOR. A decrease in GOR led to an increase in STEC. The STEC value of the system was 175 kWh/m³ at the GOR of 4 at the beginning of the experiment and increased to a stable value of 250 kWh/m³ when GOR decreased to 2.5 during the continuous-mode operation.

In addition to STEC and GOR, the SEEC of the pilot MD system in the treatment of CSG RO brine was monitored. During the continuous operation, at the water circulation rate of 450 L/h, the pressure drop over the module was stable at 0.6 bar. Given the system distillate production rate of 10 L/h during this operation and the practical efficiency of the water-circulating pump of 0.7, the SEEC of the pilot MD system was 1.1 kWh/m³. The SEEC of the pilot MD system was negligible in comparison with the STEC of 250 kWh/m³. In addition, comparing with the current state-of-the-art RO seawater desalination systems, which have an SEEC ranging from 4 to 6 kWh/m³ [39], the pilot MD system was found to consume significantly less electrical energy.

Thermal energy accounts for most of the power input into the MD process. As a result, a viable energy source for MD is waste heat available onsite (e.g., from the compressor used for liquefaction of CSG) or solar thermal energy. In Australia, the use of solar thermal energy is particularly attractive. For example, in New South Wales, the annual mean daily radiation exposure is 4.7 kWh/m² [40]. Given the solar thermal efficiency of flat-plate solar thermal collectors in the range from 0.1 to 0.8 [41], a value of 0.5 can be assumed. Thus, at the STEC value of 250 kWh/m³ and the water recovery of 80% of the MD system, a flat-plate solar thermal collector area of 85 m² is required to treat one m³/day of CSG RO brine. Taking into account a typical water recovery of 75% of the UF/RO system, the area of flat-plate solar thermal collectors required for treating one m³/day of CSG produced water is 21 m². In other words, one hectare of flat-plate solar thermal collector arrays can provide sufficient thermal energy to treat 118 m³/day of CSG RO brine, which is equivalent to 472 m³/day of raw CSG produced water. It is

noteworthy that electricity requirement for water circulation in the solar collectors has been omitted in this estimation.

4 Conclusions

Pilot treatment of CSG produced water by a combination of UF/RO and MD was demonstrated. Overall, 95% of CSG produced water could be recovered by the hybrid system for beneficial uses. The UF/RO recovered 75% fresh water from the raw CSG produced water and the pilot MD system extracted 80% fresh water from the RO brine. The low permeate flux of the pilot MD system was offset by the high packing density of the AGMD module used. Despite being operated at 80% water recovery, the distillate production rate was stable throughout the pilot study possibly because of the addition of anti-scalant to CSG produced water and the small operating temperature gradient. However, mass-balance calculation indicates the possible precipitation of silica and calcium, which may pose a scaling risk in long-term operation. When operating in continuous mode, the STEC and SEEC of the pilot MD system were stable at 250 and 1.1 kWh/m³, respectively, and a GOR of 2.5 was achieved. The integration of solar thermal energy into the MD system was considered. In New South Wales (Australia), one hectare of flat-plate solar thermal collectors can provide sufficient thermal energy for the treatment of 118 m³/d of CSG RO brine using AGMD.

Acknowledgments

The authors acknowledge the financial support of the National Centre of Excellence in Desalination Australia (which is funded by the Australian Government through the Water for the Future initiative) and AGL Energy Ltd. The authors also thank AquaStill (Sittard, the Netherlands) and OsmoFlo (Adelaide, Australia) for the loan of the pilot MD and UF/RO systems, respectively. Technical assistance from Dr Alexander Simon (University of Wollongong) and Mr Wayne Taylor (OsmoFlo) during the study is gratefully acknowledged.

References

- [1] World Energy Outlook, Are We Entering a Golden Age of Gas?, IEA, Paris, 2011, pp 1-131.
- [2] L. D. Nghiem, T. Ren, N. Aziz, I. Porter, and G. Regmi, Treatment of coal seam gas produced water for beneficial use in Australia: A review of best practices, *Desalination and Water Treatment*, 32 (2011) 316-323.
- [3] C. R. Johnston, G. F. Vance, and G. K. Ganjgunte, Irrigation with coalbed natural gas co-produced water, *Agricultural Water Management*, 95 (2008) 1243-1252.
- [4] M. H. Plumlee, J.-F. Debroux, D. Taffler, J. W. Graydon, X. Mayer, K. G. Dahm, N. T. Hancock, K. L. Guerra, P. Xu, J. E. Drewes, and T. Y. Cath, Coalbed methane produced

- water screening tool for treatment technology and beneficial use, *Journal of Unconventional Oil and Gas Resources*, 5 (2014) 22-34.
- [5] State of Queensland (Department of Natural Resources and Mines), *Forecasting coal seam gas water production in Queensland's Surat and southern Bowen basins: Summary*, 2012, pp 1-25.
- [6] P. Xu and J. E. Drewes, Viability of nanofiltration and ultra-low pressure reverse osmosis membranes for multi-beneficial use of methane produced water, *Separation and Purification Technology*, 52 (2006) 67-76.
- [7] S. Mondal and S. R. Wickramasinghe, Produced water treatment by nanofiltration and reverse osmosis membranes, *Journal of Membrane Science*, 322 (2008) 162-170.
- [8] J. E. Drewes, N. T. Hancock, K. L. Benko, K. Dahm, P. Xu, D. Heil, and T. Y. Cath, Treatment of coalbed methane produced water, *Exploration & Production/Oil and Gas Review*, 7 (2009) 126-128.
- [9] P. Xu, J. E. Drewes, and D. Heil, Beneficial use of co-produced water through membrane treatment: technical-economic assessment, *Desalination*, 225 (2008) 139-155.
- [10] State of Queensland (Department of Environment and Heritage Protection), *Coal seam gas water management policy*, Brisbane, 2012, pp 1-6.
- [11] General Electric, GE and Penrice Consortium to trial converting coal seam gas brine into saleable products, 2011, [Online] Available: <http://www.genewscenter.com/Press-Releases/GE-and-Penrice-Consortium-to-Trial-Converting-Coal-Seam-Gas-Brine-into-Saleable-Products-344a.aspx#downloads>.
- [12] A. Simon, T. Fujioka, W. E. Price, and L. D. Nghiem, Sodium hydroxide production from sodium carbonate and bicarbonate solutions using membrane electrolysis: A feasibility study, *Separation and Purification Technology*, 127 (2014) 70-76.
- [13] A. Subramani and J. G. Jacangelo, Treatment technologies for reverse osmosis concentrate volume minimization: A review, *Separation and Purification Technology*, 122 (2014) 472-489.
- [14] A. Alkudhiri, N. Darwish, and N. Hilal, Membrane distillation: A comprehensive review, *Desalination*, 287 (2012) 2-18.
- [15] B. L. Pangarkar, M. G. Sane, S. B. Parjane, and M. Guddad, Status of membrane distillation for water and wastewater treatment - A review, *Desalination and Water Treatment*, (2013) 1-20.
- [16] L. M. Camacho, L. Dumée, Z. Jianhua, L. Jun-de, M. Duke, J. Gomez, and S. Gray, Advances in membrane distillation for water desalination and purification applications, *Water* (20734441), 5 (2013) 94-196.
- [17] J.-P. Mericq, S. Laborie, and C. Cabassud, Vacuum membrane distillation of seawater reverse osmosis brines, *Water Research*, 44 (2010) 5260-5273.
- [18] K. L. Hickenbottom and T. Y. Cath, Sustainable operation of membrane distillation for enhancement of mineral recovery from hypersaline solutions, *Journal of Membrane Science*, 454 (2014) 426-435.

- [19] B. Bolto, T. Tran, and M. Hoang, Membrane distillation - A low energy desalting technique?, *Water*, 34 (2007) 59-62.
- [20] E. Drioli, F. Laganà, A. Criscuoli, and G. Barbieri, Integrated membrane operations in desalination processes, *Desalination*, 122 (1999) 141-145.
- [21] S. Adham, A. Hussain, J. M. Matar, R. Dores, and A. Janson, Application of membrane distillation for desalting brines from thermal desalination plants, *Desalination*, 314 (2013) 101-108.
- [22] X. Ji, E. Curcio, S. Al Obaidani, G. Di Profio, E. Fontananova, and E. Drioli, Membrane distillation-crystallization of seawater reverse osmosis brines, *Separation and Purification Technology*, 71 (2010) 76-82.
- [23] J. P. Mericq, S. Laborie, and C. Cabassud, Vacuum membrane distillation for an integrated seawater desalination process, *Desalination and Water Treatment*, 9 (2009) 287-296.
- [24] X. M. Li, B. Zhao, Z. Wang, M. Xie, J. Song, L. D. Nghiem, T. He, C. Yang, C. Li, and G. Chen, Water reclamation from shale gas drilling flow-back fluid using a novel forward osmosis-vacuum membrane distillation hybrid system, *Water Science and Technology*, 69 (2014) 1036-1044.
- [25] S. Lin, N. Y. Yip, and M. Elimelech, Direct contact membrane distillation with heat recovery: Thermodynamic insights from module scale modeling, *Journal of Membrane Science*, 453 (2014) 498-515.
- [26] K. W. Lawson and D. R. Lloyd, Membrane distillation, *Journal of Membrane Science*, 124 (1997) 1-25.
- [27] E. Curcio and E. Drioli, Membrane distillation and related operations - A review, *Separation and Purification Reviews*, 34 (2005) 35-86.
- [28] G. Zaragoza, A. Ruiz-Aguirre, and E. Guillén-Burrieza, Efficiency in the use of solar thermal energy of small membrane desalination systems for decentralized water production, *Applied Energy*, (2014), <http://dx.doi.org/10.1016/j.apenergy.2014.02.024>.
- [29] R. B. Saffarini, E. K. Summers, H. A. Arafat, and J. H. Lienhard V, Technical evaluation of stand-alone solar powered membrane distillation systems, *Desalination*, 286 (2012) 332-341.
- [30] E. K. Summers, H. A. Arafat, and J. H. Lienhard V, Energy efficiency comparison of single-stage membrane distillation (MD) desalination cycles in different configurations, *Desalination*, 290 (2012) 54-66.
- [31] I. J. Karassik, J. P. Messina, P. Cooper, and C. C. Heald, *Pump Handbook*, Third edition, McGraw-Hill, USA, 2001, pp . 1-1790.
- [32] K. L. Tu, L. D. Nghiem, and A. R. Chivas, Coupling effects of feed solution pH and ionic strength on the rejection of boron by NF/RO membranes, *Chemical Engineering Journal*, 168 (2011) 700-706.
- [33] A. Alkhudhiri, N. Darwish, and N. Hilal, Produced water treatment: Application of air gap membrane distillation, *Desalination*, 309 (2013) 46-51.

- [34] D. Winter, J. Koschikowski, and S. Ripperger, Desalination using membrane distillation: Flux enhancement by feed water deaeration on spiral-wound modules, *Journal of Membrane Science*, 423–424 (2012) 215-224.
- [35] J. Zhang, N. Dow, M. Duke, E. Ostarcevic, J.-D. Li, and S. Gray, Identification of material and physical features of membrane distillation membranes for high performance desalination, *Journal of Membrane Science*, 349 (2010) 295-303.
- [36] M. Gryta, Desalination of thermally softened water by membrane distillation process, *Desalination*, 257 (2010) 30-35.
- [37] F. He, K. K. Sirkar, and J. Gilron, Effects of antiscalants to mitigate membrane scaling by direct contact membrane distillation, *Journal of Membrane Science*, 345 (2009) 53-58.
- [38] C. R. Martinetti, A. E. Childress, and T. Y. Cath, High recovery of concentrated RO brines using forward osmosis and membrane distillation, *Journal of Membrane Science*, 331 (2009) 31-39.
- [39] A. Al-Karaghoul and L. L. Kazmerski, Energy consumption and water production cost of conventional and renewable-energy-powered desalination processes, *Renewable and Sustainable Energy Reviews*, 24 (2013) 343-356.
- [40] Australian Government (Bureau of Meteorology), Daily global solar exposure, [Online] Available: <http://www.bom.gov.au>.
- [41] S. A. Kalogirou, Solar thermal collectors and applications, *Progress in Energy and Combustion Science*, 30 (2004) 231-295.
- [42] J. Koschikowski, M. Wiegghaus, M. Rommel, V. S. Ortin, B. P. Suarez, and J. R. Betancort Rodríguez, Experimental investigations on solar driven stand-alone membrane distillation systems for remote areas, *Desalination*, 248 (2009) 125-131.
- [43] F. Banat, N. Jwaied, M. Rommel, J. Koschikowski, and M. Wiegghaus, Desalination by a “compact SMADES” autonomous solar-powered membrane distillation unit, *Desalination*, 217 (2007) 29-37.
- [44] J. Koschikowski, M. Wiegghaus, and M. Rommel, Solar thermal-driven desalination plants based on membrane distillation, *Desalination*, 156 (2003) 295-304.

List of tables

Table 1. Characteristics of the spiral-wound AGMD module.

Total net membrane surface area (m ²)	7.2
Diameter of the module (m)	0.4
Height of the module (m)	0.5
Length of envelope (m)	1.5
Width of envelope (m)	0.4
Thickness of flow channels (mm)	2.0
Number of evaporator channels	6
Number of condenser channels	6
Number of distillate channels	12

Table 2. Characteristics of water before and after the pilot UF/RO treatment of CSG produced water.

	Raw CSG water	RO permeate	RO brine
General characteristics			
Conductivity (μS/cm)	6,550	110	21,800
Total dissolved solids (g/L)	3.57	0.06	14.10
Turbidity (NTU)	6.1	0.07	0.22
pH	8.2	6.8	8.2
SAR	103	-	-
Ion concentration (mg/L)			
Sodium	1,710	18	6,840
Bicarbonate	1,920	0	4,740
Chloride	1,400	15	5,520
Magnesium	5	0	17
Potassium	8	0	32
Calcium	10	1	14
Iron	0	0	0
Silica	13	1	75

Table 3. Characteristics of water before and after the pilot MD treatment of CSG RO brine.

	RO brine	MD distillate	MD brine	Concentration Factor
General characteristics				
Conductivity (mS/cm)	21.8	0.5	82.1	4
Total dissolved solids (g/L)	14.10	0.25	86.10	6.1
Turbidity (NTU)	0.22	0.11	0.67	-
pH	8.2	6.3	8.2	-
Ion concentration (mg/L)				
Sodium	6,840	65	34,200	5
Bicarbonate	4,740	110	32,800	6.9
Chloride	5,520	63	31,800	5.8
Magnesium	17	nd	74	4.4
Aluminium	nd	nd	nd	-
Potassium	32	1	146	4.6
Calcium	14	nd	34	2.4
Iron	nd	nd	nd	-
Silica	75	5	170	2

nd: not detectable.

Table 4. Comparisons between the pilot MD system used in the present study and other pilot MD systems reported in literature.

	Present study	Literature			
		[42]	[43]	[28]	[44]
Permeate flux (L/m ² h)	2.1	2.1	2.5	3.4	1.88
Water circulation flow rate (L/h)	450	280-415	400	500	200-400
Feed temperature at evaporator inlet (°C)	55	60-85	-	85	60-85
STEC (kWh/m ³)	175-250	100-200	200-300	250-600	140-200
GOR	2.5-4	3-6	0.3-0.9	-	4-6

List of figures

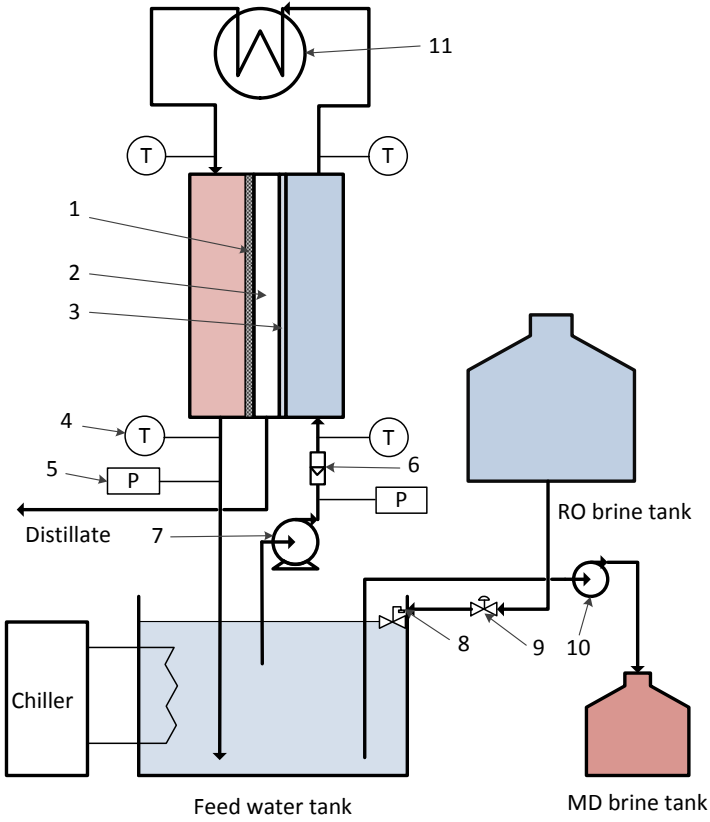


Fig. 1. Schematic diagram of the CSG RO brine treatment by the pilot MD system: (1) membrane, (2) air gap, (3) condenser, (4) temperature sensors; (5) pressure sensors, (6) flow meter, (7) water-circulating pump, (8) float valve, (9) one-way valve, (10) peristaltic pump, (11) heat exchanger.

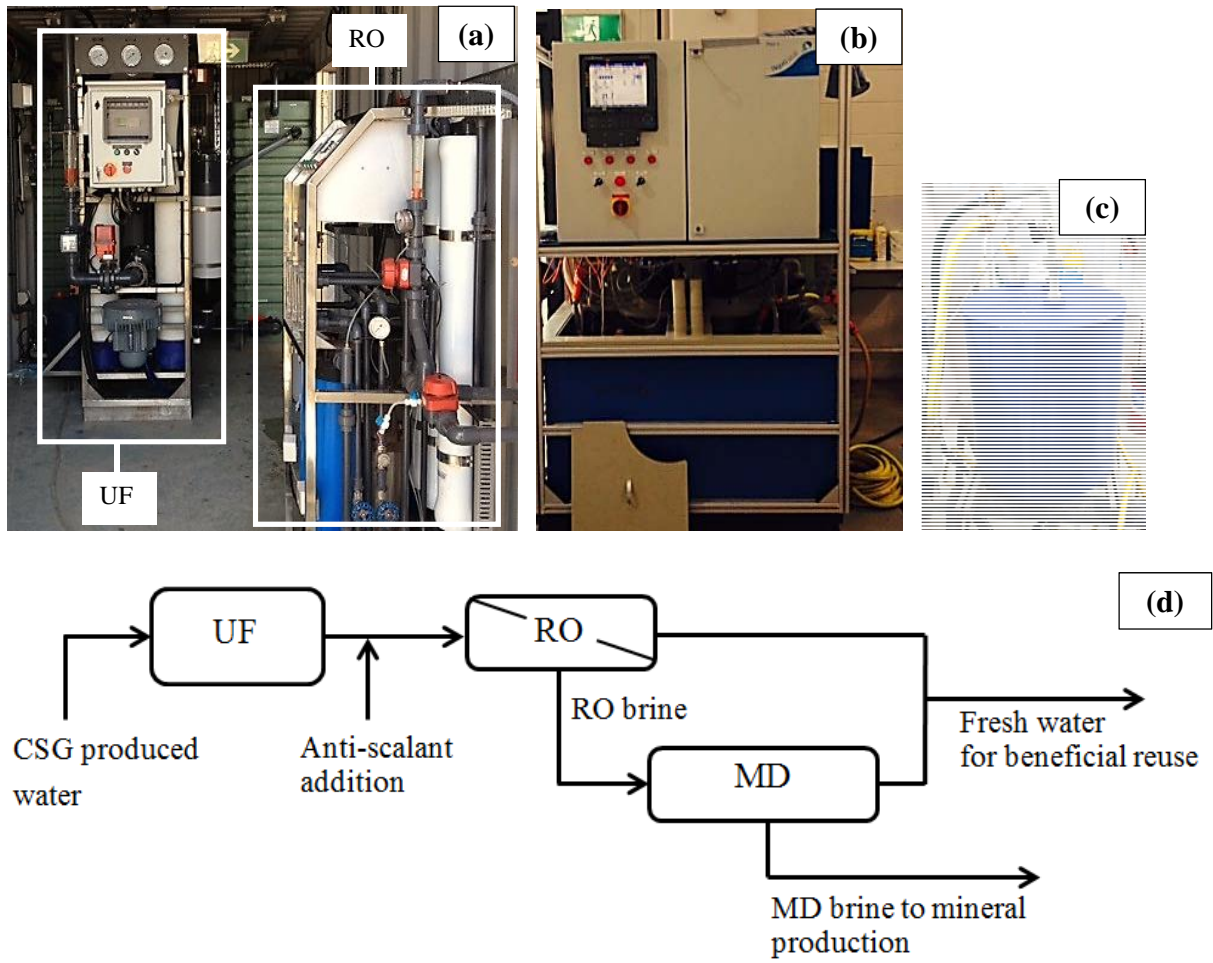


Fig. 2. The treatment process of CSG produced water; (a) UF and RO pilot systems, (b) MD pilot system, (c) Spiral-wound AGMD membrane module, (d) Schematic diagram of the treatment process.

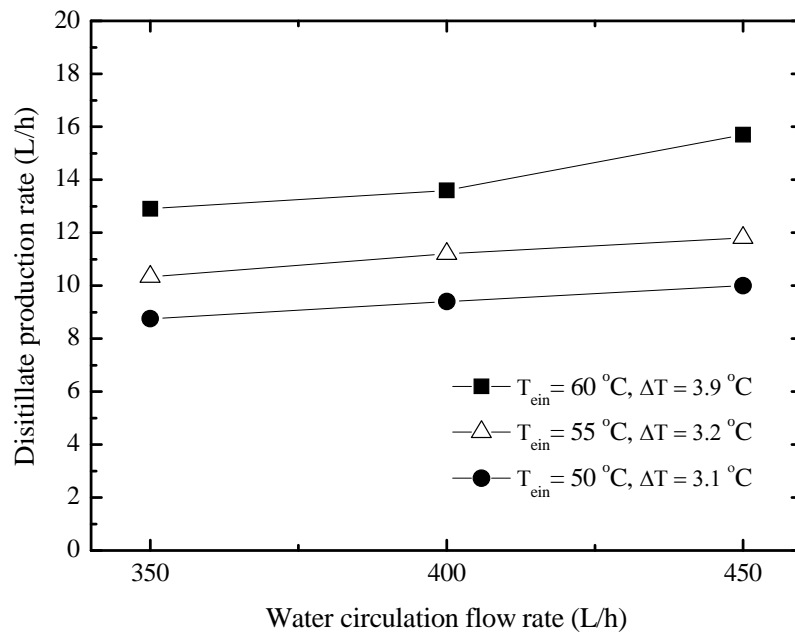


Fig. 3. Distillate production rate of the pilot MD system at various evaporator inlet temperatures (T_{ein}) and water circulation flow rates. Feed solution was 8000 mg/L sodium chloride.

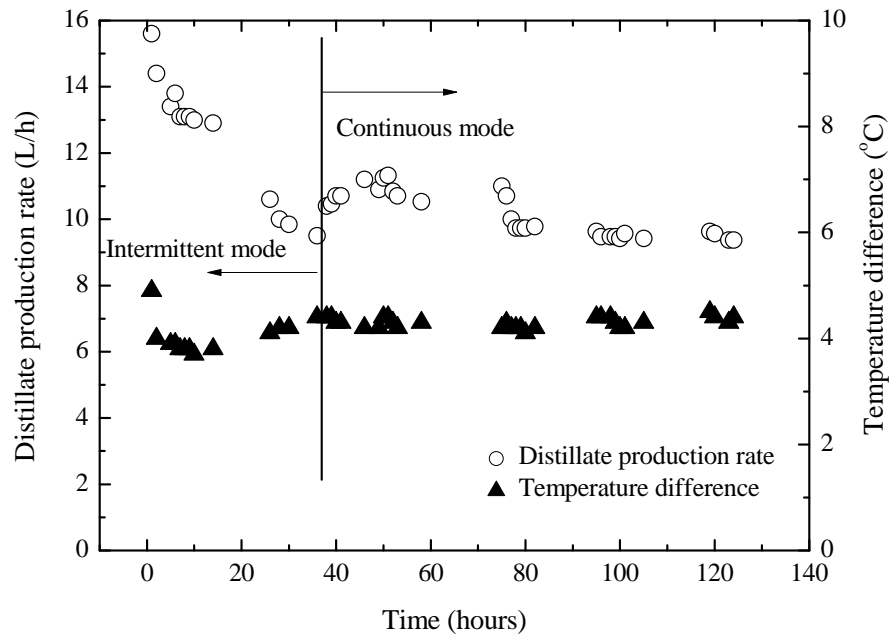


Fig. 4. Distillate production rate and temperature difference as a function of time during the pilot MD treatment process of CSG RO brine (The condenser inlet temperature $T_{cin} = 25\text{ }^{\circ}\text{C}$; the evaporator inlet temperature $T_{cin} = 55\text{ }^{\circ}\text{C}$; water circulation flow rate $F = 450\text{ L/h}$).

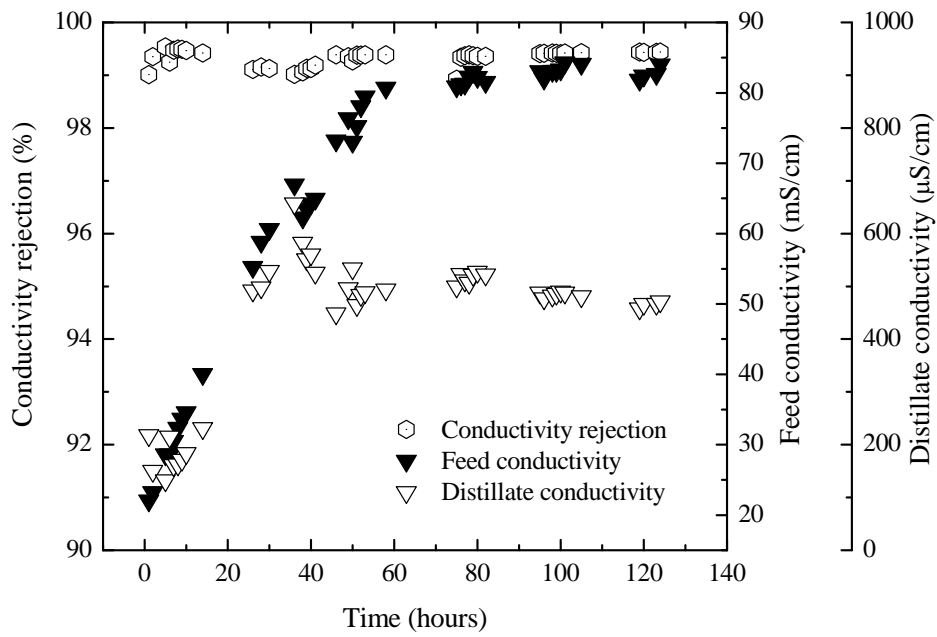


Fig. 5. Conductivity rejection of the pilot MD system and conductivities of its feed and distillate during the treatment of CSG RO brine.

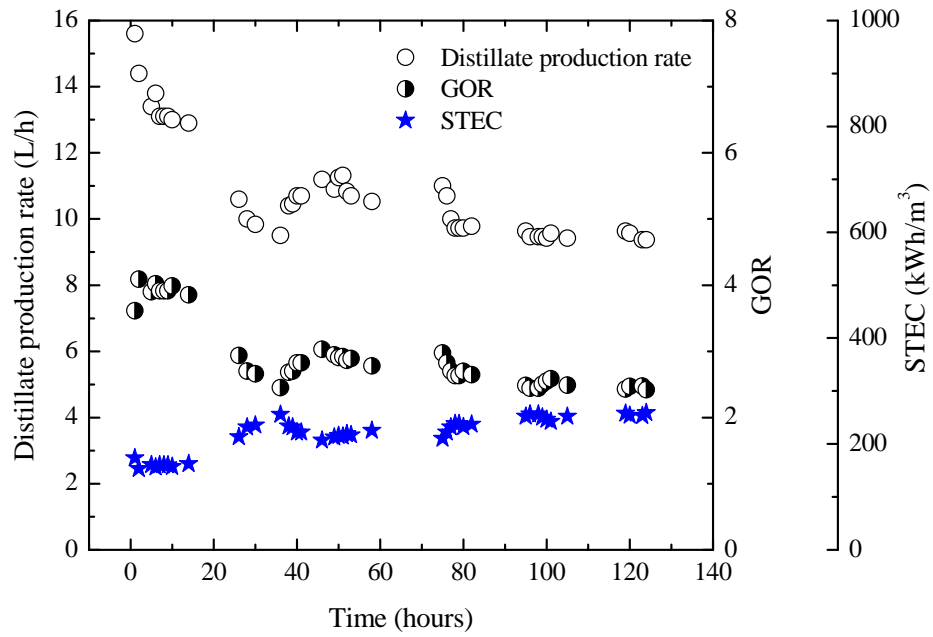


Fig. 6. Distillate production rate, GOR, and STEC as a function of time during the treatment of CSG RO brine by the pilot MD system ($T_{\text{ein}} = 55 \text{ }^\circ\text{C}$, $T_{\text{cin}} = 25 \text{ }^\circ\text{C}$, $F = 450 \text{ L/h}$).